

# Reheating in tachyonic inflationary models: Effects on the large scale curvature perturbations

Rajeev Kumar Jain<sup>1\*</sup>, Pravabati Chingangbam<sup>2†</sup>, and L. Sriramkumar<sup>1‡</sup>

<sup>1</sup>*Harish-Chandra Research Institute, Chhatnag Road, Jhansi, Allahabad 211 019, India.*

<sup>2</sup>*Korea Institute for Advanced Study, 207-43 Cheongnyangni 2-dong, Dongdaemun-gu, Seoul 130-722, Republic of Korea.*

We investigate the problem of perturbative reheating and its effects on the evolution of the curvature perturbations in tachyonic inflationary models. We derive the equations governing the evolution of the scalar perturbations for a system consisting of a tachyon and a perfect fluid. Assuming the perfect fluid to be radiation, we solve the coupled equations for the system numerically and study the evolution of the perturbations from the sub-Hubble to the super-Hubble scales. In particular, we analyze the effects of the transition from tachyon driven inflation to the radiation dominated epoch on the evolution of the large scale curvature and non-adiabatic pressure perturbations. We consider two different potentials to describe the tachyon and study the effects of two possible types of decay of the tachyon into radiation. We plot the spectrum of curvature perturbations at the end of inflation as well as at the early stages of the radiation dominated epoch. We find that reheating does not affect the amplitude of the curvature perturbations in any of these cases. These results corroborate similar conclusions that have been arrived at earlier based on the study of the evolution of the perturbations in the super-Hubble limit. We illustrate that, before the transition to the radiation dominated epoch, the relative non-adiabatic pressure perturbation between the tachyon and radiation decays in a fashion very similar to that of the intrinsic entropy perturbation associated with the tachyon. Moreover, we show that, after the transition, the relative non-adiabatic pressure perturbation dies down extremely rapidly during the early stages of the radiation dominated epoch. It is these behavior which ensure that the amplitude of the curvature perturbations remain unaffected during reheating. We also discuss the corresponding results for the popular chaotic inflation model in the case of the canonical scalar field.

PACS numbers: 98.80.Cq

Keywords: Inflationary models, Cosmological perturbation theory, Reheating

## I. EFFECTS OF INFLATIONARY AND POST-INFLATIONARY DYNAMICS ON THE EVOLUTION OF THE SUPER-HUBBLE PERTURBATIONS

In the standard inflationary scenario, the scales of cosmological interest exit the Hubble radius within the first few (about 8-10)  $e$ -folds of inflation and, hence, are outside the Hubble scale during the later epochs. When comparing the predictions of the inflationary models with the Cosmic Microwave Background (CMB) and the large scale structure data, it is often assumed that the amplitude of the curvature perturbations remain constant at super-Hubble scales. In such a situation, the observed CMB anisotropies directly determine the amplitude and the shape of the perturbation spectrum imprinted on the modes when they left the Hubble radius during inflation. Typically, the amplitude of the perturbations constrain the parameters that describe the inflaton potential, while the shape of the spectrum limits its form (see any of the standard texts [1] or one of the following reviews [2]).

Provided inflation is of the slow roll type for *all* of the required number of  $e$ -folds, it is indeed true that the amplitude of the curvature perturbations freeze at their value at Hubble exit. However, if there is a period of deviation from slow roll inflation, then the asymptotic (i.e. the extreme super-Hubble) amplitude of the modes that leave the Hubble radius just before the deviation are enhanced when compared to their value at Hubble exit [3]. While modes that leave well before the deviation remain unaffected, it is found that there exists an intermediate range of modes whose amplitudes are actually suppressed at super-Hubble scales [4, 5]. Depending on the form of the departure from slow roll, these effects lead to certain features in the scalar perturbation spectrum. If such deviations occur either during or soon after the cosmological scales leave the Hubble radius, then the CMB observations constrain the resulting features rather well (for an inexhaustive list, see Ref. [6]). But, at smaller scales, only theoretical tools are currently available

---

\* Present address: Département de Physique Théorique and Center for Astroparticle Physics, Université de Genève, 24 Quai Ernest-Ansermet, CH-1211 Genève 4, Switzerland. E-mail: rajeev.jain@unige.ch

† Present address: Indian Institute of Astrophysics, II Block, Koramangala, Bangalore 560034, India. E-mail: prava@iiap.res.in

‡ Present address: Department of Physics, Indian Institute of Technology Madras, Chennai 600036, India. E-mail: sri-ram@physics.iitm.ac.in

to restrict the form of the primordial spectrum. These constraints are essentially based on the number density of primordial black holes that are formed towards the end of inflation (for recent discussions in this context, see, for example, Ref. [7]).

Since the cosmological scales are well outside the Hubble radius by the early stages of inflation, clearly, the *shape* of the perturbation spectrum on such large scales is indeed unlikely to be affected by subsequent dynamics. But, over the past decade, it has been recognized that post-inflationary dynamics can alter the *amplitude* of the curvature perturbations at super-Hubble scales, in particular, when more than one component of matter is present. Preheating, the curvaton scenario and the modulated reheating mechanism are popular examples that illustrate the interesting possibilities of post-inflationary dynamics. Preheating—a mechanism that transfers energy from the inflaton to radiation through an explosive production of quanta corresponding to an intermediate scalar field—is known to even lead to an exponential growth in the amplitude of the super-Hubble perturbations (for the earlier discussions, see Ref. [8] and, for more recent efforts, see, for instance, Ref. [9]). In the curvaton scenario, while the inflationary epoch still remains the source of the perturbations, these perturbations are amplified after inflation due to the presence of entropic perturbations (see, for example, Ref. [10]). The modulated reheating scenario is an extreme case wherein inflation is essentially required only to resolve the horizon problem, whereas the perturbations are generated due to an inhomogeneous decay rate when the energy is being transferred from the inflaton to radiation through other fields [11–13]. These different alternatives indicate that the post-inflationary evolution of the large scale curvature perturbations can be highly model dependent and, therefore, requires a careful and systematic study. Evidently, in these scenarios, the effects of post-inflationary dynamics have to be taken into account when constraining the inflationary models using the CMB observations (in this context, see, for instance, Ref. [14]).

With these motivations in mind, in this paper, we investigate the problem of the more conventional (perturbative) reheating scenario [15–17], and its effects on the evolution of the curvature perturbations in tachyonic inflationary models (for the original discussions on the tachyon, see Refs. [18, 19]; for efforts on treating the tachyon as an inflaton, see, for instance, Refs. [20–22]; for discussions on reheating in such inflationary models, see Refs. [23, 24]). We shall consider two types of potentials to describe the tachyon and construct scenarios of transition from inflation to radiation domination for the following two possible cases of the decay rate  $\Gamma$  of the tachyon into radiation: (i) a constant, and (ii) dependent on the tachyon. We solve the coupled equations for the system numerically and study the evolution of the perturbations from the sub-Hubble to the super-Hubble scales. Importantly, we shall consider the effects of the transition from inflation to the radiation dominated epoch on the evolution of the large scale (i.e. those that correspond to cosmological scales today) curvature and non-adiabatic pressure (i.e. the intrinsic entropy as well as the relative entropy or the isocurvature) perturbations. We shall evaluate the spectrum of curvature perturbations at the end of inflation as well as at the early stages of the radiation dominated epoch. As we shall illustrate, reheating does not affect the amplitude of the curvature perturbations in any of these cases. We shall also show that, before the transition to the radiation dominated epoch, the relative non-adiabatic pressure perturbation between the tachyon and radiation decays in a fashion very similar to that of the intrinsic entropy perturbation associated with the tachyon. Moreover, we demonstrate that, after the transition, the relative non-adiabatic pressure perturbation dies down extremely rapidly during the early stages of the radiation dominated epoch. It is these behavior which ensure that the amplitude of the curvature perturbations remains unaffected during reheating. Our results corroborate similar conclusions that have been arrived at earlier in the literature based on the study of the evolution of the perturbations in the super-Hubble limit [11]. We shall also discuss similar effects in the case of the canonical scalar field.

A few clarifying remarks are in order at this stage of the discussion. We should stress that the set up we are considering is the standard cold inflationary scenario, followed by an epoch of reheating achieved by the standard method of introducing a coarse-grained decay rate in the equation of motion describing the inflaton [15, 16]. Recently, an analysis somewhat similar to what we shall consider here has been studied in the context of warm inflationary scenarios involving tachyonic fields [25]. Though there can exist similarities in the form of the equations in the cold and the warm inflationary scenarios, the physics in these two scenarios are rather different (for a recent discussion, see, for example, Ref. [26]). Moreover, to analyze the effects of reheating on the large scale perturbations, one could have possibly studied the evolution of the perturbations in the super-Hubble limit, say, the first order (in time) differential equations usually considered in the literature (cf. Refs. [11, 12, 27]). However, some concerns have been raised that the coupling between the inflaton and radiation may affect the amplitude as well as the scalar spectral index in certain situations [16, 17]. Also, the modified background dynamics preceding reheating can effect the extent of small scale primordial black holes that are formed towards the end of inflation. If we are to address such issues, it requires that we study the evolution of the perturbations from the sub-Hubble to the super-Hubble scales. We shall comment further on some of these points in the concluding section.

The remainder of this paper is organized as follows. In the following section, we shall summarize the essential background equations for the system consisting of the tachyon and a perfect fluid and set up scenarios of transition from inflation to radiation domination. In Sec. III, we shall obtain the equations describing the scalar perturbations for the system of the tachyon and a perfect fluid. In Sec. IV, we shall evolve the coupled system of equations describing

the perturbations and study the effects of the transition from inflation to the radiation dominated epoch on the super-Hubble curvature perturbations. We shall plot the spectrum of curvature perturbations at the end of inflation as well as at the early stages of the radiation dominated epoch. We shall also explicitly illustrate that the intrinsic entropy perturbation associated with the tachyon and the relative non-adiabatic pressure perturbation between the tachyon and radiation decay in a similar fashion before and after the transition to the radiation dominated epoch. It is the behavior of these non-adiabatic pressure perturbations which ensure that the amplitude of the curvature perturbations remains unaffected during reheating. Finally, in Sec. V, we conclude with a summary and a discussion on the results we have obtained. In the appendix, we shall discuss the corresponding results for the chaotic inflation model in the case of the canonical scalar field.

The notations and conventions we shall adopt are as follows. We shall set  $\hbar = c = 1$ , but shall display  $G$  explicitly, and define the Planck mass to be  $M_{\text{Pl}} = (8\pi G)^{-1/2}$ . We shall work with the metric signature of  $(+, -, -, -)$ . We shall express the various quantities in terms of the cosmic time  $t$ , and we shall denote differentiation with respect to  $t$  by an overdot. While we shall use the subscript  $i$  to denote the spatial components of, say, the momentum flux associated with the matter fields, the subscripts  $\alpha$  and  $\beta$  shall refer to the two components of matter.

## II. THE TRANSITION FROM TACHYON DRIVEN INFLATION TO THE RADIATION DOMINATED EPOCH

In this section, we shall discuss the background equations describing the evolution of the tachyon that is interacting with a perfect fluid. Assuming the perfect fluid to be radiation, we shall construct scenarios of transition from tachyon driven inflation to radiation domination for the following two possible types of the decay rate  $\Gamma$  [cf. Eq. (8) below] of the inflaton into radiation: (i) a constant, and (ii) dependent on the tachyon [11].

### A. Background equations in the presence of interacting components

Consider a  $(3+1)$ -dimensional, spatially flat, smooth, expanding, Friedmann universe described by the line element

$$ds^2 = dt^2 - a^2(t) d\mathbf{x}^2, \quad (1)$$

where  $t$  denotes the cosmic time and  $a(t)$  is the scale factor. Let  $\rho$  and  $p$  denote the total energy density and the total pressure of a system consisting of multiple components of fields and fluids that are driving the expansion. Then, the Einstein's equations corresponding to the above line-element lead to the following Friedmann equations for the scale factor  $a(t)$ :

$$H^2 = \left(\frac{8\pi G}{3}\right) \rho \quad \text{and} \quad \dot{H} = -(4\pi G)(\rho + p), \quad (2)$$

where  $H = (\dot{a}/a)$  is the Hubble parameter. Also, the conservation of the total energy of the system leads to the continuity equation

$$\dot{\rho} + 3H(\rho + p) = 0. \quad (3)$$

The total energy density and the total pressure of the system can be expressed as the sum of the energy density  $\rho_\alpha$  and the pressure  $p_\alpha$  of the individual components as follows:

$$\rho = \sum_{\alpha} \rho_{\alpha} \quad \text{and} \quad p = \sum_{\alpha} p_{\alpha}. \quad (4)$$

If the different components of fields and fluids do not interact, then, in addition to the total energy density, the energy density of the individual components will be conserved as well. Hence, in such a situation, the energy density  $\rho_\alpha$  of each component will individually satisfy the continuity equation

$$\dot{\rho}_{\alpha} + 3H(\rho_{\alpha} + p_{\alpha}) = 0. \quad (5)$$

On the other hand, when the different components interact, the continuity equation for the individual components can be expressed as (see, for instance, Refs. [11, 28, 29])

$$\dot{\rho}_{\alpha} + 3H(\rho_{\alpha} + p_{\alpha}) = Q_{\alpha}, \quad (6)$$

where  $Q_\alpha$  denotes the rate at which energy density is transferred to the component  $\alpha$  from the other components. The conservation of the energy of the complete system then leads to the following constraint on the total rate of transfer of the energy densities:

$$\sum_{\alpha} Q_{\alpha} = 0. \quad (7)$$

### B. The case of the tachyon and a perfect fluid

Let us now consider the system of a tachyon (which we shall denote as  $T$ ) that is interacting with a perfect fluid (referred to, hereafter, as  $F$ ), so that  $\alpha = (T, F)$ . We shall assume that the rate at which energy density is transferred to the perfect fluid, i.e.  $Q_F$ , is given by [24]

$$Q_F = \Gamma \dot{T}^2 \rho_T, \quad (8)$$

where  $\rho_T$  is the energy density of the tachyon. Such a transfer of energy is assumed to describe—albeit, in a course grained fashion—the perturbative decay of the tachyon into particles that constitute the perfect fluid. The quantity  $\Gamma$  represents the corresponding decay rate and, as we shall discuss below, it can either be a constant or depend on the tachyon [11].

For the above  $Q_F$ , the continuity equation (6) corresponding to the perfect fluid is given by

$$\dot{\rho}_F + 3H(1 + w_F)\rho_F = \Gamma \dot{T}^2 \rho_T, \quad (9)$$

where  $w_F = (p_F/\rho_F)$  is the equation of state parameter describing the perfect fluid, which we shall assume to be a constant. Also, it is evident from Eq. (7) that

$$Q_T = -Q_F = -\Gamma \dot{T}^2 \rho_T. \quad (10)$$

Therefore, the continuity equation for the tachyon energy density  $\rho_T$  reduces to

$$\dot{\rho}_T + 3H(\rho_T + p_T) = -\Gamma \dot{T}^2 \rho_T, \quad (11)$$

where  $p_T$  is the pressure associated with the tachyon. Given a potential  $V(T)$  describing the tachyon, the corresponding energy density  $\rho_T$  and pressure  $p_T$  are given by (see, for instance, Refs. [4, 21, 22])

$$\rho_T = \left( \frac{V(T)}{\sqrt{1 - \dot{T}^2}} \right) \quad \text{and} \quad p_T = -V(T) \sqrt{1 - \dot{T}^2}. \quad (12)$$

On substituting these two expressions in the continuity equation (11), we arrive at the following equation of motion for the tachyon  $T$  [24]:

$$\left( \frac{\ddot{T}}{1 - \dot{T}^2} \right) + 3H\dot{T} + \Gamma\dot{T} + \left( \frac{V_T}{V} \right) = 0, \quad (13)$$

where  $V_T \equiv (dV/dT)$ .

Before we proceed, the following clarification on the choice of  $Q_F$  in Eq. (8) is in order at this stage of the discussion. Recall that, in a situation wherein the canonical scalar field, say  $\phi$ , drives inflation, it is common to introduce a  $(\Gamma\dot{\phi})$  term in the field equation to describe the perturbative decay of the inflaton [see Refs. [1, 2, 15–17], also see Eq. (A4)]. Motivated by the canonical case, the choice of  $Q_F$  in Eq. (8) has been specifically made so as to lead to the  $(\Gamma\dot{T})$  term in the equation of motion (13) for the tachyon [24]. Needless to add, the choice (8) is but one of the many possibilities that can help in achieving reheating at the end of inflation.

### C. Tachyonic inflationary models, different possible $\Gamma$ and reheating

In this sub-section, assuming the perfect fluid to be radiation with  $w_F = (1/3)$ , we shall construct specific scenarios of transition from tachyon driven inflation to an epoch of radiation domination.

We shall consider two different types of potentials in order to describe the tachyon.

- The first potential we shall consider is given by

$$V_1(T) = \left( \frac{\lambda}{\cosh(T/T_0)} \right), \quad (14)$$

a potential that is well motivated from the string theory perspective [19].

- Our second choice will be the following phenomenologically motivated power law potential that has been considered earlier in the literature (see, for example, Ref. [21]):

$$V_2(T) = \left( \frac{\lambda}{1 + (T/T_0)^4} \right). \quad (15)$$

In order to achieve the necessary amount of inflation and the correct amplitude for the scalar perturbations, suitable values for the two parameters  $\lambda$  and  $T_0$  that describe the above potentials can be arrived at as follows. Firstly, one finds that, in these potentials, inflation typically occurs around  $T \simeq T_0$  corresponding to an energy scale of about  $\lambda^{1/4}$ . Secondly, it turns out that, the quantity  $(\lambda T_0^2/M_{\text{pl}}^2)$  has to be much larger than unity for the potential slow roll parameters to be small and thereby ensure that, at least, 60  $e$ -folds of inflation takes place. Therefore, one first chooses a sufficiently large value of  $(\lambda T_0^2/M_{\text{pl}}^2)$  by hand in order to guarantee slow roll. The COBE normalization condition for the scalar perturbations then provides the second constraint, thereby determining the values of both the parameters  $\lambda$  and  $T_0$  [21].

In the absence of the fluid, we find that the two potentials  $V_1(T)$  and  $V_2(T)$  above allow about 60  $e$ -folds of slow roll inflation and lead to the correct COBE amplitude for the choice of the parameters and initial conditions listed in Table I. Also, in such a situation, it is known that, at the end of inflation, the tachyon leads to an epoch of dust like

Potential	$\lambda$	$T_0$	$(T_i/T_0)$	$\dot{T}_i$
$V_1(T)$	$10^{-6}$	$10^9$	5.81	0.1
$V_2(T)$	$10^{-5.15}$	$3.7 \times 10^4$	4.56	0.1

TABLE I: Achieving inflation: The values for the parameters of the tachyon potential and the initial conditions for the inflaton (the initial value  $T_i$  of the tachyon and its initial velocity  $\dot{T}_i$ ) that we work with. These choices for the parameters and initial conditions lead to the required 60  $e$ -folds of slow roll inflation and the observed amplitude for the scalar perturbations.

behavior [20, 21], thereby making a radiation dominated epoch difficult to achieve. However, as we shall illustrate below, when the tachyon is interacting with the fluid, we can ensure that a transition from inflation to the radiation dominated regime occurs with a suitable choice of the amplitude for the decay rate  $\Gamma$ .

As we mentioned before, we shall consider the following two possible choices for the decay rate  $\Gamma$ : (i)  $\Gamma_1 = \mathcal{A} = \text{constant}$ , and (ii)  $\Gamma_2 = \Gamma(T)$ . We shall work with the following specific form of  $\Gamma(T)$ :

$$\Gamma_2 = \Gamma(T) = \mathcal{A} \left( 1 - \mathcal{B} \tanh [(T - \mathcal{C})/\mathcal{D}] \right), \quad (16)$$

where  $\mathcal{A}$ ,  $\mathcal{B}$ ,  $\mathcal{C}$  and  $\mathcal{D}$  are constants that we shall choose suitably to achieve the desired evolution. (It turns out that the above form of  $\Gamma(T)$  prove to be convenient in the numerical calculations, helping us illustrate the required behavior. We shall comment further on this choice in the concluding section.) We find that a transition from inflation to radiation domination can be achieved provided the amplitude of  $\Gamma$  (viz.  $\mathcal{A}$ ) is chosen to be less than the Hubble parameter  $H$  (which is almost a constant) during the epoch of slow roll inflation. In Table II, we have listed the values of the initial energy density of radiation (viz.  $\rho_\gamma^i$ ) and the various parameters describing the decay rates (for the tachyon, we have used the same values listed in Table I) that lead to about 60  $e$ -folds of slow roll inflation, the correct scalar amplitude, while also reheating the universe within 2-3  $e$ -folds after the end of inflation. In the left column of Fig. 1, we have plotted the fractional contributions (with respect to the total energy density) of the energy densities of the tachyon and radiation, i.e.  $\Omega_T = (\rho_T/\rho)$  and  $\Omega_\gamma = (\rho_\gamma/\rho)$ , as a function of the number of  $e$ -folds  $N$  for the potential  $V_1(T)$ . It is evident from the figure that the two choices for the decay rate  $\Gamma$  ensure the completion of reheating (i.e.  $\Omega_\gamma \simeq 1$ ) within a couple of  $e$ -folds after the end of inflation. In the right column of the figure, we have plotted the corresponding effective equation of state parameter, viz.  $w = (p/\rho)$ , and also the first Hubble slow roll parameter, viz.  $\epsilon = -(\dot{H}/H^2)$ , of the entire system, for the same tachyon potential. These plots, while confirming that inflation has indeed ended and reheating has been realized, also indicate the nature of the composite matter during the transition. We should add that a very similar behavior occurs for the potential  $V_2(T)$ .

Potential	$\Gamma$	$\rho_\gamma^i$	$\mathcal{A}$	$\mathcal{B}$	$\mathcal{C}$	$\mathcal{D}$
$V_1(T)$	$\Gamma_1$	$10^{-40}$	$5\lambda$	–	–	–
	$\Gamma_2$	$10^{-40}$	$5\lambda$	$10^{-2}$	$2T_0$	$T_0$
$V_2(T)$	$\Gamma_1$	$10^{-40}$	$1.43 \times 10^{-2} \lambda$	–	–	–
	$\Gamma_2$	$10^{-40}$	$10^{-2} \lambda$	$10^{-2}$	$2T_0$	$T_0$

TABLE II: Achieving inflation *and* reheating: The values of the initial energy density of radiation  $\rho_\gamma^i$  and the parameters describing the decay rates that we work with when the interaction of the tachyon with radiation is taken into account. For the tachyon, we use the same values listed in the previous table. These parameters and initial conditions lead to about 60  $e$ -folds of slow roll inflation, the required amplitude for the perturbations, and also reheat the universe within a couple of  $e$ -folds after inflation.

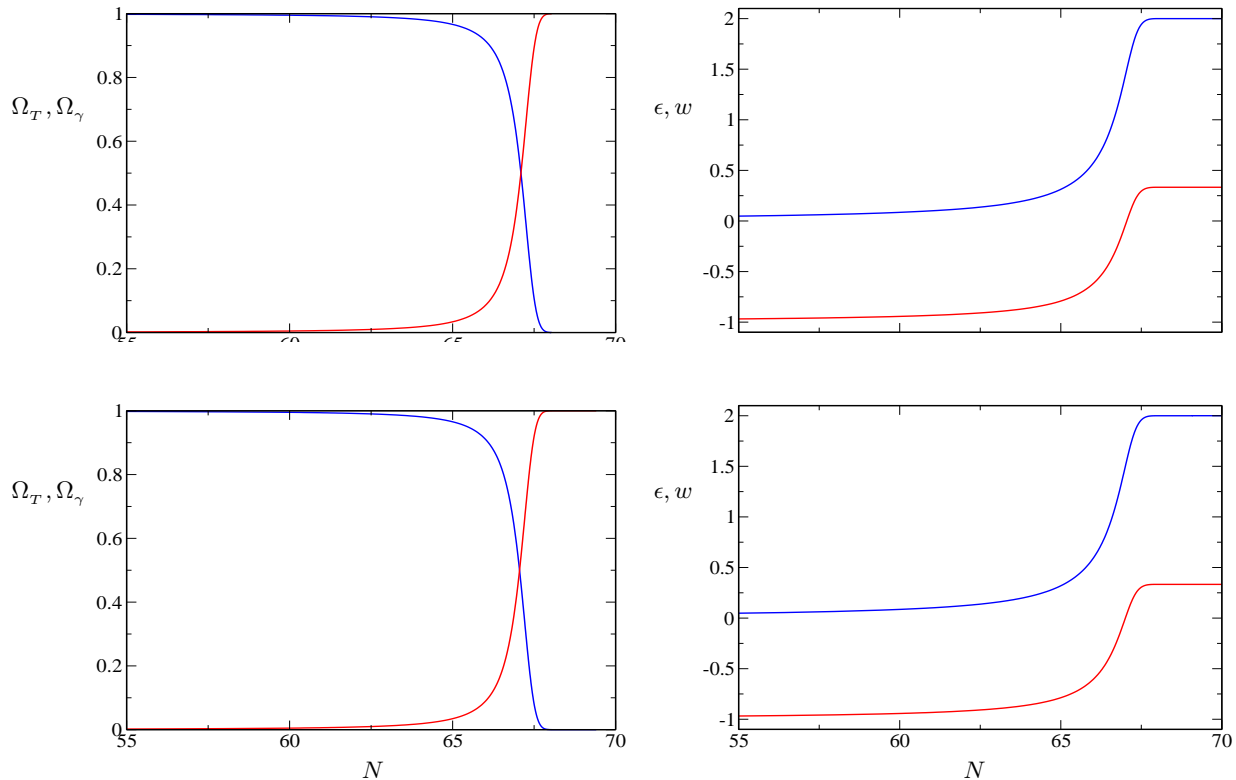


FIG. 1: In the left column, the evolution of the quantities  $\Omega_T$  (in blue) and  $\Omega_\gamma$  (in red) has been plotted as a function of the number of  $e$ -folds  $N$  for the tachyon potential  $V_1(T)$  and the two cases of  $\Gamma$ , viz.  $\Gamma_1 = \text{constant}$  (on top) and  $\Gamma_2 = \Gamma(T)$  (at the bottom), with  $\Gamma(T)$  given by Eq. (16). Similarly, in the right system column, the evolution of the first Hubble slow roll parameter  $\epsilon$  (in blue) and the equation of state parameter of the entire system  $w$  (in red) has been plotted as a function of the number of  $e$ -folds for the same potential and the different cases of  $\Gamma$ , as indicated above. All these plots correspond to the values for the various parameters and the initial conditions that we have listed in Tables I and II. The figures clearly illustrate the transfer of energy from the inflaton to radiation. (Note that  $\epsilon = 2$  during the radiation dominated epoch.) We have chosen the various parameters in such a fashion that there is a sufficiently rapid transition from inflation to radiation domination without any intermediate regime, as suggested by the evolution of  $\epsilon$  and  $w$ . We find that a very similar behavior occurs for the potential  $V_2(T)$ .

### III. EQUATIONS OF MOTION GOVERNING THE SCALAR PERTURBATIONS FOR THE SYSTEM

In this section, using the first order Einstein's equations and the equations describing the conservation of the perturbed energy density of the tachyon and the perfect fluid, we shall arrive at the coupled, second order (in time) differential equations governing the scalar perturbations for the system consisting of the tachyon and the fluid. For convenience, we shall work in the uniform curvature gauge (UCG), a gauge that is also referred to, often, as the

spatially flat gauge.

### A. First order Einstein's equations

If we take into account the scalar perturbations to the spatially flat background metric (1), then, in the UCG, the Friedmann line-element is given by [1, 2]

$$ds^2 = (1 + 2A) dt^2 - 2a(\partial_i B) dx_i dt - a^2(t) d\mathbf{x}^2, \quad (17)$$

where  $A$  and  $B$  are functions that describe the two degrees of freedom associated with the perturbations. Being a scalar field, the tachyon, evidently, does not possess any anisotropic stress at the linear order in the perturbations. We shall assume that the perfect fluid does not contain any anisotropic stress either. In such a case, at the first order in the perturbations, Einstein's equations in the UCG can be written as [1, 2]

$$-3H^2 A - \left(\frac{H}{a}\right) \nabla^2 B = (4\pi G) \delta\rho, \quad (18)$$

$$H(\partial_i A) = (4\pi G)(\partial_i \delta q), \quad (19)$$

$$H\dot{A} + (2\dot{H} + 3H^2)A = (4\pi G)\delta p, \quad (20)$$

where the quantities  $\delta\rho$ ,  $(\partial_i \delta q)$ , and  $\delta p$  denote the perturbations in the total energy density, the total momentum flux, and the total pressure of the complete system, respectively. The absence of the anisotropic stress leads to the following additional relation between the two functions  $A$  and  $B$  describing the scalar perturbations:

$$A + a(\dot{B} + 2HB) = 0. \quad (21)$$

For the system of our interest, viz. that of the tachyon and a perfect fluid described by a constant equation of state parameter  $w_F$ , the quantities  $\delta\rho$ ,  $\delta q$  and  $\delta p$  are given by

$$\delta\rho = (\delta\rho_T + \delta\rho_F) = \left(\frac{V_T \delta T}{\sqrt{1 - \dot{T}^2}}\right) + \left(\frac{V\dot{T}}{(1 - \dot{T}^2)^{3/2}}\right) (\delta\dot{T} - A\dot{T}) + \delta\rho_F, \quad (22)$$

$$\delta q = (\delta q_T + \delta q_F) = \left(\frac{V\dot{T}\delta T}{\sqrt{1 - \dot{T}^2}}\right) - \psi_F, \quad (23)$$

$$\delta p = (\delta p_T + \delta p_F) = -\left(V_T \delta T \sqrt{1 - \dot{T}^2}\right) + \left(\frac{V\dot{T}}{\sqrt{1 - \dot{T}^2}}\right) (\delta\dot{T} - A\dot{T}) + w_F \delta\rho_F, \quad (24)$$

where  $\delta T$  denotes the perturbation in the tachyon and  $\psi_F$  is proportional to the potential that determines the three (i.e. the spatial) velocity of the perfect fluid<sup>1</sup>.

### B. Equations of motion describing the perturbed matter components

In the UCG, at the first order in the perturbations, the equation describing the conservation of the energy density of the component  $\alpha$  is given by [2, 27–29]

$$\dot{\delta\rho}_\alpha + 3H(\delta\rho_\alpha + \delta p_\alpha) - \left(\frac{1}{a^2}\right) \nabla^2 [\delta q_\alpha + (\rho_\alpha + p_\alpha) a B] - Q_\alpha A - \delta Q_\alpha = 0, \quad (25)$$

---

<sup>1</sup> Usually, for a perfect fluid, the quantity  $\delta q_F$  is written as  $[(\rho_F + p_F)\chi_F]$ , where  $\chi_F$  is the potential whose spatial gradient describes the three velocity of the fluid (see, for instance, Refs. [1, 2]). For convenience, we have instead defined the entire quantity  $[(\rho_F + p_F)\chi_F]$  as  $-\psi_F$  [16]. As we shall point out later, we have ensured that suitable sub-Hubble initial conditions are imposed on  $\psi_F$ .

where the quantities  $\delta\rho_\alpha$ ,  $\delta q_\alpha$  and  $\delta p_\alpha$  denote the perturbations at the linear order in the energy density, the momentum flux, and the pressure of the particular component  $\alpha$ , while  $Q_\alpha$  and  $\delta Q_\alpha$  indicate the rate at which the energy is transferred to the component  $\alpha$  and the perturbation in the rate, respectively. The equation of motion that governs the perturbation  $\delta T$  in the tachyon can now be obtained upon using the expressions (22)–(24) for  $\delta\rho_T$ ,  $\delta q_T$  and  $\delta p_T$  in above equation for the conservation of the perturbed energy density. We find that the equation of motion describing the perturbation  $\delta T$  is given by

$$\begin{aligned} & \left( \frac{\delta\dot{T}}{1-\dot{T}^2} \right) + \left[ (3H + \Gamma) (1 - 3\dot{T}^2) - 2\dot{T} \left( \frac{V_T}{V} \right) \right] \left( \frac{\delta\dot{T}}{1-\dot{T}^2} \right) + \left[ \left( \frac{d^2 \ln V}{dT^2} \right) - \left( \frac{1}{a^2} \right) \nabla^2 \right] \delta T \\ & - \left( \frac{\dot{T} \dot{A}}{1-\dot{T}^2} \right) + \left[ 6H\dot{T}^3 + 2 \left( \frac{V_T}{V} \right) + \Gamma \dot{T} (1 + \dot{T}^2) \right] \left( \frac{A}{1-\dot{T}^2} \right) - \left( \frac{\dot{T}}{a} \right) (\nabla^2 B) + \dot{T} \delta\Gamma = 0, \end{aligned} \quad (26)$$

where  $\delta\Gamma$  denotes the first order perturbation in the decay rate. Upon using Eq. (25), we find that the equation describing the conservation of the perturbed energy density of the fluid  $\delta\rho_F$  can be written as

$$\begin{aligned} & \delta\dot{\rho}_F + 3H(1 + w_F) \delta\rho_F + \left( \frac{1}{a^2} \right) \nabla^2 \psi_F - \left( \frac{\Gamma V \dot{T} (2 - \dot{T}^2)}{(1 - \dot{T}^2)^{3/2}} \right) \delta\dot{T} - \left( \frac{\Gamma V_T \dot{T}^2}{\sqrt{1 - \dot{T}^2}} \right) \delta T \\ & + \left( \frac{\Gamma V \dot{T}^2}{(1 - \dot{T}^2)^{3/2}} \right) A - \left( \frac{(1 + w_F) \rho_F}{a} \right) \nabla^2 B - \left( \frac{V \dot{T}^2}{\sqrt{1 - \dot{T}^2}} \right) \delta\Gamma = 0. \end{aligned} \quad (27)$$

Also, on using Einstein's equations (19) and (20), we obtain the following first order (in time) differential equation for the quantity  $\psi_F$  that describes the spatial velocity of the fluid:

$$\dot{\psi}_F + 3H\psi_F + w_F \delta\rho_F + (1 + w_F) \rho_F A + \left( \frac{\Gamma V \dot{T}}{\sqrt{1 - \dot{T}^2}} \right) \delta T = 0. \quad (28)$$

We should emphasize here that the above equations take into account the two possibilities of  $\Gamma$  (i.e. it can either be a constant or depend on the tachyon) that we had discussed earlier.

### C. The coupled perturbation variables and the initial conditions

The variables describing the perturbations in the tachyon and the fluid that we shall eventually evolve numerically are [2, 16]

$$\mathcal{Q}_T = \delta T \quad \text{and} \quad \mathcal{Q}_F = \left( \frac{\psi_F}{\sqrt{(1 + w_F) \rho_F}} \right). \quad (29)$$

We have already obtained a second order differential equation (in time) describing the evolution of  $\mathcal{Q}_T$  [viz. Eq. (26)]. A similar equation for  $\mathcal{Q}_F$  can be obtained by differentiating Eq. (28) with respect to time, and upon using Eq. (27) that describes the conservation of the perturbed energy density of the fluid. Then, on utilizing the first order Einstein's equations (18), (19) and (21) to eliminate the scalar metric perturbations  $A$  and  $B$ , we can arrive at a set of coupled, second order (in time, again!) differential equations for the quantities  $\mathcal{Q}_T$  and  $\mathcal{Q}_F$ .

For simplicity, let us first discuss the case wherein the decay rate  $\Gamma$  is a constant. We shall later indicate as to how certain coefficients in the differential equations change when  $\Gamma$  is assumed to be dependent on the tachyon. Upon suitably using the background equations (2), (9) and (13), we find that the differential equations satisfied by the perturbation variables  $\mathcal{Q}_T$  and  $\mathcal{Q}_F$  can be written as

$$\ddot{\mathcal{Q}}_\alpha + \sum_\beta \left( \mathcal{F}_{\alpha\beta} \dot{\mathcal{Q}}_\beta + \mathcal{G}_{\alpha\beta} \mathcal{Q}_\beta \right) = 0, \quad (30)$$



where, as before,  $(\alpha, \beta) = (T, F)$ . The coefficients  $\mathcal{F}_{\alpha\beta}$  and  $\mathcal{G}_{\alpha\beta}$  appearing in the above equations are given by

$$\mathcal{F}_{TT} = (3H + \Gamma) (1 - 3\dot{T}^2) - 2\dot{T} \left( \frac{V_T}{V} \right), \quad (31)$$

$$\mathcal{F}_{TF} = \left( \frac{4\pi G}{H} \right) \left[ 1 - \left( \frac{1 - \dot{T}^2}{w_F} \right) \right] \dot{T} \sqrt{(1 + w_F) \rho_F}, \quad (32)$$

$$\mathcal{F}_{FT} = \left( \frac{V\dot{T}}{\sqrt{1 - \dot{T}^2}} \right) \left[ \left( \frac{4\pi G}{H} \right) \left\{ 1 - \left( \frac{w_F}{1 - \dot{T}^2} \right) \right\} \sqrt{(1 + w_F) \rho_F} + \left\{ 1 + w_F \left( \frac{2 - \dot{T}^2}{1 - \dot{T}^2} \right) \right\} \left( \frac{\Gamma}{\sqrt{(1 + w_F) \rho_F}} \right) \right], \quad (33)$$

$$\mathcal{F}_{FF} = 3H + \left( \frac{\Gamma V \dot{T}^2}{\sqrt{1 - \dot{T}^2}} \right) \left( \frac{1}{\rho_F} \right), \quad (34)$$

$$\begin{aligned} \mathcal{G}_{TT} &= (1 - \dot{T}^2) \left[ \left( \frac{d^2 \ln V}{dT^2} \right) - \left( \frac{1}{a^2} \right) \nabla^2 \right] \\ &+ \left( \frac{4\pi G}{H} \right) \left( \frac{V\dot{T}}{\sqrt{1 - \dot{T}^2}} \right) \left[ (2 - \dot{T}^2) \left( \frac{2V_T}{V} \right) + (2 + \dot{T}^2) (3H + \Gamma) \dot{T} - \left( \frac{\Gamma\dot{T}}{w_F} \right) (1 - \dot{T}^2) \right] \\ &- \left( \frac{4\pi G}{H} \right)^2 \left[ \left( \frac{2V^2\dot{T}^4}{1 - \dot{T}^2} \right) - \left( \frac{V\dot{T}^2}{\sqrt{1 - \dot{T}^2}} \right) \left\{ 1 + \left( \frac{1 - \dot{T}^2}{w_F} \right) \right\} (1 + w_F) \rho_F \right], \end{aligned} \quad (35)$$

$$\begin{aligned} \mathcal{G}_{TF} &= \left( \frac{4\pi G}{H} \right) \left[ - \left( \frac{3H\dot{T}}{2} \right) \left\{ 1 + \left( \frac{1 - \dot{T}^2}{w_F} \right) \right\} (1 + w_F) + \left( \frac{1}{2\rho_F} \right) \left\{ 1 - \left( \frac{1 - \dot{T}^2}{w_F} \right) \right\} \left( \frac{\Gamma V \dot{T}^3}{\sqrt{1 - \dot{T}^2}} \right) \right. \\ &- \left. \left\{ 6H\dot{T}^3 + 2 \left( \frac{V_T}{V} \right) + (\Gamma\dot{T}) (1 + \dot{T}^2) \right\} \sqrt{(1 + w_F) \rho_F} \right. \\ &+ \left. \left( \frac{4\pi G}{H} \right)^2 \left[ \left( \frac{2V\dot{T}^3}{\sqrt{1 - \dot{T}^2}} \right) + \left\{ 1 + \left( \frac{1 - \dot{T}^2}{w_F} \right) \right\} \dot{T} [(1 + w_F) \rho_F] \right] \sqrt{(1 + w_F) \rho_F}, \end{aligned} \quad (36)$$

$$\begin{aligned} \mathcal{G}_{FT} &= - \left( \frac{4\pi G}{H} \right) \left[ \left\{ 1 + \left( \frac{w_F}{1 - \dot{T}^2} \right) \right\} [(1 + w_F) \rho_F] V_T \sqrt{1 - \dot{T}^2} \right. \\ &+ \left. \left( \frac{3HV\dot{T}}{\sqrt{1 - \dot{T}^2}} \right) (1 + w_F)^2 \rho_F - \left( \frac{\Gamma V^2 \dot{T}^3}{1 - \dot{T}^2} \right) \left\{ 1 - \left( \frac{w_F \dot{T}^2}{1 - \dot{T}^2} \right) \right\} \right] \left( \frac{1}{\sqrt{(1 + w_F) \rho_F}} \right) \\ &- \left( \frac{4\pi G}{H} \right)^2 \left[ \left( \frac{V^2 \dot{T}^3}{1 - \dot{T}^2} \right) \left\{ 1 + \left( \frac{w_F}{1 - \dot{T}^2} \right) \right\} [(1 + w_F) \rho_F] - \left( \frac{2V\dot{T}}{\sqrt{1 - \dot{T}^2}} \right) [(1 + w_F) \rho_F]^2 \right] \left( \frac{1}{\sqrt{(1 + w_F) \rho_F}} \right) \\ &+ \left( \frac{\Gamma V}{\sqrt{1 - \dot{T}^2}} \right) \left[ \left( \frac{V_T}{V} \right) (1 - \dot{T}^2) - \left( \frac{V_T}{V} \right) w_F \dot{T}^2 + \Gamma \dot{T} - 3H w_F \dot{T} \right] \left( \frac{1}{\sqrt{(1 + w_F) \rho_F}} \right), \end{aligned} \quad (37)$$

$$\begin{aligned} \mathcal{G}_{FF} &= - \left( \frac{w_F}{a^2} \right) \nabla^2 + \left( \frac{9H^2}{4} \right) (1 - w_F^2) \\ &+ \left( \frac{4\pi G}{H} \right) \left[ \left( \frac{3H}{2} \right) (1 + w_F) (1 + 3w_F) \rho_F + \left( \frac{3H}{2} \right) \left( \frac{V\dot{T}^2}{\sqrt{1 - \dot{T}^2}} \right) (w_F - 1) - \left( \frac{\Gamma V \dot{T}^2}{\sqrt{1 - \dot{T}^2}} \right) \left\{ 1 - \left( \frac{w_F \dot{T}^2}{1 - \dot{T}^2} \right) \right\} \right] \\ &- \left( \frac{4\pi G}{H} \right)^2 \left[ \left( \frac{V\dot{T}^2}{\sqrt{1 - \dot{T}^2}} \right) \left\{ 1 + \left( \frac{w_F}{1 - \dot{T}^2} \right) \right\} [(1 + w_F) \rho_F] + 2[(1 + w_F) \rho_F]^2 \right] \\ &- \left( \frac{\Gamma V \dot{T}}{\sqrt{1 - \dot{T}^2}} \right) \left[ \left( \frac{\Gamma\dot{T}}{2\rho_F} \right) (2 - \dot{T}^2) + \left( \frac{V_T}{V} \right) \left( \frac{1 - \dot{T}^2}{\rho_F} \right) - \left( \frac{3H\dot{T}}{2\rho_F} \right) (w_F + \dot{T}^2) + \left( \frac{\Gamma V \dot{T}^3}{4\rho_F^2 \sqrt{1 - \dot{T}^2}} \right) \right]. \end{aligned} \quad (38)$$

As we had pointed out, the coefficients  $\mathcal{F}_{\alpha\beta}$  and  $\mathcal{G}_{\alpha\beta}$  above have been derived assuming that the decay rate  $\Gamma$  is a constant. For the case wherein the decay rate is a function of the tachyon, the coefficients  $\mathcal{G}_{TT}$  and  $\mathcal{G}_{FT}$  are modified

to

$$\mathcal{G}_{TT} \rightarrow \mathcal{G}_{TT} + (1 - \dot{T}^2) \dot{T} \Gamma_T, \quad (39)$$

$$\mathcal{G}_{FT} \rightarrow \mathcal{G}_{FT} + \left( \frac{V \dot{T}^2}{\sqrt{1 - \dot{T}^2}} \right) \left( \frac{w_F}{\sqrt{(1 + w_F) \rho_F}} \right) \Gamma_T, \quad (40)$$

where  $\Gamma_T \equiv (d\Gamma/dT)$ . The other coefficients remain unaffected in this case.

We should mention here that we have checked that we indeed recover the standard equations in the different limiting cases from the coupled equations (30) for  $\mathcal{Q}_T$  and  $\mathcal{Q}_F$ . For instance, when the fluid is ignored and the decay rate is assumed to vanish, the equation for the variable  $\mathcal{Q}_T$  reduces to the equation that has been derived earlier in the literature for describing the perturbation in the tachyon (see, for instance, Refs. [4, 21, 25]). Moreover, when the tachyon is assumed to vanish and its coupling to the fluid is also ignored, we find that we arrive at the well-known equation governing the fluid perturbation, as required [1, 2].

#### IV. EFFECTS OF REHEATING ON THE SCALAR POWER SPECTRUM

In this section, we shall discuss the effects of reheating on the large scale curvature perturbations and the scalar power spectrum. We shall also investigate the behavior of the non-adiabatic pressure perturbations at large scales, when reheating is achieved through the two different choices for the decay rate.

##### A. Evolution of the curvature perturbations and the scalar power spectrum

We shall solve the coupled equations (30) for the two variables  $\mathcal{Q}_T$  and  $\mathcal{Q}_F$  numerically. Imposing the standard Bunch-Davies initial conditions, we shall evolve the perturbations from the sub-Hubble to the super-Hubble scales, and analyse the effects of the transition from inflation to the radiation dominated epoch on the evolution of the large scale perturbations. We shall compute the scalar power spectrum at the end of inflation and soon after reheating is complete. Let us begin by quickly summarizing the essential quantities of interest and the initial conditions that we shall be imposing.

Let  $\mathcal{R}_T$  and  $\mathcal{R}_F$  denote the curvature perturbations associated with the tachyon and the fluid, respectively. We find that these curvature perturbations are related to the variables  $\mathcal{Q}_T$  and  $\mathcal{Q}_F$  as follows [2, 4, 21, 25]:

$$\mathcal{R}_T = \left( \frac{H}{\dot{T}} \right) \delta T = \left( \frac{H}{\dot{T}} \right) \mathcal{Q}_T, \quad (41)$$

$$\mathcal{R}_F = - \left( \frac{H}{\rho_F + p_F} \right) \psi_F = - \left( \frac{H}{\sqrt{(1 + w_F) \rho_F}} \right) \mathcal{Q}_F. \quad (42)$$

The total curvature perturbation of the system, say,  $\mathcal{R}$ , can then be expressed as a weighted sum of the individual curvature perturbations in the following fashion (see, for instance, Refs. [28, 29]):

$$\mathcal{R} = \sum_{\alpha} \left( \frac{\rho_{\alpha} + p_{\alpha}}{\rho + p} \right) \tilde{\mathcal{R}}_{\alpha}. \quad (43)$$

Therefore, for our system of interest, the total curvature perturbation is given by

$$\mathcal{R} = H \left[ \left( \frac{V \dot{T}^2}{\sqrt{1 - \dot{T}^2}} \right) + [(1 + w_F) \rho_F] \right]^{-1} \left[ \left( \frac{V \dot{T}}{\sqrt{1 - \dot{T}^2}} \right) \mathcal{Q}_T - \sqrt{[(1 + w_F) \rho_F]} \mathcal{Q}_F \right]. \quad (44)$$

The scalar power spectrum is then defined in terms of the Fourier mode  $\mathcal{R}_k$  of the total curvature perturbation as

$$\mathcal{P}_s(k) = \left( \frac{k^3}{2\pi^2} \right) |\mathcal{R}_k|^2. \quad (45)$$

The Mukhanov-Sasaki variables, say,  $v_T$  and  $v_F$ , associated with the tachyon and the fluid are related to the corresponding curvature perturbations as follows:

$$v_T = (\mathcal{R}_T z_T) \quad \text{and} \quad v_F = (\mathcal{R}_F z_F), \quad (46)$$

where the quantities  $z_T$  and  $z_F$  are given by [1, 2, 4, 21]

$$z_T = \left( \frac{3}{8\pi G} \right)^{1/2} \left( \frac{a\dot{T}}{\sqrt{1-\dot{T}^2}} \right) \quad \text{and} \quad z_F = \left( \frac{a}{H} \right) \left[ \frac{(1+w_F)\rho_F}{w_F} \right]^{1/2}. \quad (47)$$

As is usually done, we shall impose the following initial conditions on the Fourier modes of the perturbation variables  $v_T$  and  $v_F$ :

$$v_k = \left( \frac{1}{2\omega_k} \right)^{1/2} \quad \text{and} \quad \dot{v}_k = - \left( \frac{i}{a} \right) \left( \frac{\omega_k}{2} \right)^{1/2}, \quad (48)$$

where

$$\omega_k^2 = \left[ (k c_s)^2 - a^2 \{ (\ddot{z}/z) + (H \dot{z}/z) \} \right], \quad (49)$$

with  $c_s^2 = (1 - \dot{T}^2)$  in the case of the tachyon and  $c_s^2 = w_F$  in the case of the fluid. Also, we shall impose these conditions when the modes are well inside the Hubble radius during the inflationary epoch. We shall transform these initial conditions to the corresponding conditions on the variables  $\mathcal{Q}_T$  and  $\mathcal{Q}_F$  when numerically integrating the coupled equations (30).

We shall focus on modes that correspond to cosmological scales today. We shall choose our parameters in such a fashion that modes spread over four orders of magnitude (say,  $10^{-4} \lesssim k \lesssim 1 \text{ Mpc}^{-1}$ ) leave the Hubble radius during the early stages of inflation (they actually leave during  $5 \lesssim N \lesssim 15$ ). As we have discussed earlier, for our choice of the parameters and initial conditions on the background variables, reheating is achieved after about 65 odd  $e$ -folds (also see Fig. 1). Moreover, the transition from inflation to radiation domination occurs within about 2-3  $e$ -folds after inflation has terminated. We evaluate the scalar power spectrum towards the end of inflation as well as soon after the transition to the radiation dominated epoch is complete. In the left column of Fig. 2, we have plotted the evolution of the amplitudes of the individual (viz.  $|\mathcal{R}_T|$  and  $|\mathcal{R}_\gamma|$  corresponding to the tachyon and radiation, respectively) as well as the total curvature perturbation (i.e.  $|\mathcal{R}|$ ) for a typical cosmological scale (we have chosen  $k = 0.1 \text{ Mpc}^{-1}$ ) across the transition from inflation to radiation domination. And, in the right column of the figure, we have plotted the scalar power spectrum (constructed out of the total curvature perturbation) evaluated before and after the transition. It is evident from the plots that the amplitude of the total curvature perturbation remains unaffected during reheating when the decay rate  $\Gamma$  is either a constant or is a function of the tachyon. These results confirm similar conclusions that have been arrived at earlier based on the first order (in time) super-Hubble equations [11].

## B. Evolution of the entropy perturbations

In this section, we shall discuss the evolution of the entropic (i.e. the non-adiabatic pressure) perturbations across the transition from inflation to the radiation dominated epoch.

Let us recall the key quantities and equations. In the UCG, the gauge invariant Bardeen potential  $\Phi$  is given by

$$\Phi = A + a \left( \dot{B} + H B \right). \quad (50)$$

Upon using the first order Einstein's equations (18), (20) and (21), it can be shown that the Bardeen potential satisfies the differential equation [1, 2]

$$\ddot{\Phi} + (4 + 3c_A^2) H \dot{\Phi} + \left[ 2\dot{H} + 3H^2 (1 + c_A^2) \right] \Phi - \left( \frac{c_A^2}{a^2} \right) \nabla^2 \Phi = (4\pi G) \delta p^{\text{NA}}, \quad (51)$$

where  $c_A^2 = (\dot{p}/\dot{\rho})$  denotes the adiabatic speed of sound in the composite system, and the quantity  $\delta p^{\text{NA}}$  is the non-adiabatic pressure perturbation defined as

$$\delta p^{\text{NA}} = (\delta p - c_A^2 \delta \rho). \quad (52)$$

Using Einstein's equations (19) and (21), the total curvature perturbation  $\mathcal{R}$  of the system can be written in terms of the Bardeen potential  $\Phi$  as follows [1, 2]:

$$\mathcal{R} = \Phi + \left( \frac{2\rho}{3H} \right) \left( \frac{\dot{\Phi} + H\Phi}{\rho + p} \right). \quad (53)$$

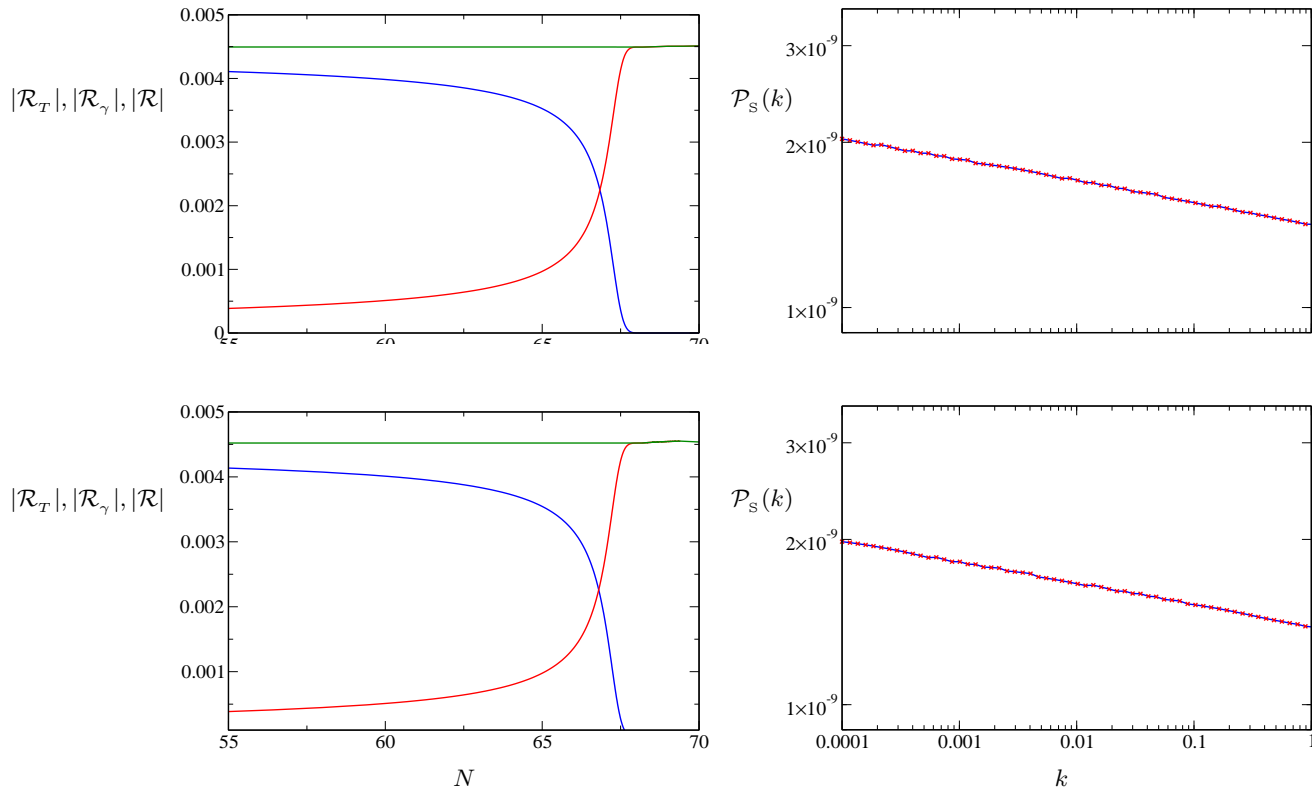


FIG. 2: In the left column, the evolution of the amplitudes of the curvature perturbations associated with the tachyon ( $|\mathcal{R}_T|$ , in blue) and radiation ( $|\mathcal{R}_\gamma|$ , in red) as well as the weighted sum of the two ( $|\mathcal{R}|$ , in green) has been plotted as a function of the number of  $e$ -folds  $N$  for the two possible cases of  $\Gamma$ , viz.  $\Gamma_1 = \text{constant}$  (on top) and  $\Gamma_2 = \Gamma(T)$  (at the bottom). In these plots, we have chosen a typical cosmological scale with the wavenumber  $k = 0.1 \text{ Mpc}^{-1}$ . Clearly, the amplitude of the total curvature perturbation remains constant across the transition in both the cases. In the right column, the scalar power spectrum has been plotted towards the end of inflation (in blue) and soon after complete reheating has been achieved (in red) for the two cases of  $\Gamma$ , as mentioned above. These plots unambiguously illustrate that the amplitude of the nearly scale invariant power spectrum is unaffected in both the cases. (In these plots, the blue line lies right beneath the red one!) Note that all these plots correspond to the potential  $V_1(T)$  with values for the various parameters and the initial conditions that are listed in Tables I and II. We find that a very similar behavior occurs for the potential  $V_2(T)$ .

On substituting this expression for the curvature perturbation in Eq. (51) that governs the evolution of the Bardeen potential  $\Phi$  and making use of the background equations, one can arrive at the well-known equation

$$\dot{\mathcal{R}} = - \left( \frac{H}{\dot{H}} \right) \left[ (4\pi G) \delta p^{\text{NA}} + \left( \frac{c_A^2}{a^2} \right) \nabla^2 \Phi \right]. \quad (54)$$

This equation clearly suggests that, at super-Hubble scales, any change in the amplitude of the curvature perturbations has to be due to the non-trivial evolution of the non-adiabatic pressure perturbation  $\delta p^{\text{NA}}$ .

The perfect fluid, by definition, does not possess any intrinsic entropy perturbation. Therefore, the non-adiabatic pressure perturbation  $\delta p^{\text{NA}}$  of our composite system depends on the intrinsic non-adiabatic pressure perturbation of the tachyon, say,  $\delta p_T^{\text{NA}}$ , and the relative non-adiabatic pressure perturbation between the tachyon and the perfect fluid (i.e. the isocurvature perturbation), which we shall denote as  $\delta p_{TF}^{\text{NA}}$ . Hence, we can write

$$\delta p^{\text{NA}} = (\delta p_T^{\text{NA}} + \delta p_{TF}^{\text{NA}}), \quad (55)$$

where the quantity  $\delta p_{TF}^{\text{NA}}$  is defined as (see, for instance, Ref. [4])

$$\delta p_{TF}^{\text{NA}} = (\delta p_T - c_T^2 \delta \rho_T) \quad (56)$$

with  $c_T^2 = (\dot{p}_T/\dot{\rho}_T)$ . The relative non-adiabatic pressure perturbation  $\delta p_{TF}^{\text{NA}}$  is then given by (see, for instance, Refs. [11, 30, 31])

$$\delta p_{TF}^{\text{NA}} = (3H + \Gamma) (w_F - c_T^2) \left( \frac{\rho_T + p_T}{\rho + p} \right) [(\rho_F + p_F) - (\Gamma/3H)(\rho_T + p_T)] \left[ \left( \frac{\delta \rho_T}{\dot{\rho}_T} \right) - \left( \frac{\delta \rho_F}{\dot{\rho}_F} \right) \right]. \quad (57)$$

Upon using the expressions (22) and (24), and Einstein's equations (18), (20) and (21), we find that we can write the quantities  $\delta \rho_T$ ,  $\delta p_T$  and  $\delta \rho_F$  in terms of the variables  $\mathcal{Q}_T$  and  $\mathcal{Q}_F$  as follows:

$$\begin{aligned} \delta \rho_T &= \left[ \left( \frac{V_T}{\sqrt{1 - \dot{T}^2}} \right) - \left( \frac{4\pi G}{H} \right) \left( \frac{V^2 \dot{T}^3}{(1 - \dot{T}^2)^2} \right) \right] \mathcal{Q}_T + \left( \frac{V \dot{T}}{(1 - \dot{T}^2)^{3/2}} \right) \dot{\mathcal{Q}}_T \\ &+ \left( \frac{4\pi G}{H} \right) \left( \frac{V \dot{T}^2}{(1 - \dot{T}^2)^{3/2}} \right) \sqrt{(1 + w_F) \rho_F} \mathcal{Q}_F, \end{aligned} \quad (58)$$

$$\begin{aligned} \delta p_T &= - \left[ V_T \sqrt{1 - \dot{T}^2} + \left( \frac{4\pi G}{H} \right) \left( \frac{V^2 \dot{T}^3}{1 - \dot{T}^2} \right) \right] \mathcal{Q}_T + \left( \frac{V \dot{T}}{\sqrt{1 - \dot{T}^2}} \right) \dot{\mathcal{Q}}_T \\ &+ \left( \frac{4\pi G}{H} \right) \left( \frac{V \dot{T}^2}{\sqrt{1 - \dot{T}^2}} \right) \sqrt{(1 + w_F) \rho_F} \mathcal{Q}_F, \end{aligned} \quad (59)$$

$$\begin{aligned} \delta \rho_F &= - \left[ \left( \frac{4\pi G}{H} \right) \left( \frac{V \dot{T}}{\sqrt{1 - \dot{T}^2}} \right) (1 + w_F) \left( \frac{\rho_F}{w_F} \right) + \left( \frac{\Gamma V \dot{T}}{w_F \sqrt{1 - \dot{T}^2}} \right) \right] \mathcal{Q}_T \\ &- \left[ \left( \frac{3H}{2w_F} \right) (1 - w_F) \sqrt{(1 + w_F) \rho_F} + \left( \frac{\Gamma V \dot{T}^2}{\sqrt{1 - \dot{T}^2}} \right) \left( \frac{1 + w_F}{4w_F^2 \rho_F} \right)^{1/2} - \left( \frac{4\pi G}{H} \right) \left( \frac{1}{w_F} \right) [(1 + w_F) \rho_F]^{3/2} \right] \mathcal{Q}_F \\ &- \left( \frac{1}{w_F} \right) \sqrt{(1 + w_F) \rho_F} \dot{\mathcal{Q}}_F. \end{aligned} \quad (60)$$

These three relations allow us to express the non-adiabatic pressure perturbations  $\delta p_T^{\text{NA}}$  and  $\delta p_{TF}^{\text{NA}}$  in terms of  $\mathcal{Q}_T$ ,  $\mathcal{Q}_F$ , and their time derivatives.

In Fig. 3, we have plotted the amplitudes of the Bardeen potential (i.e.  $|\Phi|$ ) and the non-adiabatic pressure perturbations (viz.  $|\delta p_T^{\text{NA}}|$  and  $|\delta p_{T\gamma}^{\text{NA}}|$ ) as a function of the number of  $e$ -folds. For convenience in numerical computation, we have chosen a very small scale mode (corresponding to  $k = 10^{16} \text{ Mpc}^{-1}$ ) that leaves the Hubble radius around 58  $e$ -folds or so during inflation<sup>2</sup>. The following points are evident from these two plots. To begin with, barring a very small change in its amplitude—which is expected during the transition from inflation to the radiation dominated epoch—the Bardeen potential  $\Phi$  remains a constant at super-Hubble scales. Secondly, it is clear from the plots that the intrinsic entropy perturbation associated with the tachyon  $|\delta p_T^{\text{NA}}|$  decays as  $e^{-(2N)}$  at super-Hubble scales during inflation, a result that is well known in the literature (see, for instance, Refs. [3, 4]). Lastly, and interestingly, we find that the isocurvature perturbation  $|\delta p_{T\gamma}^{\text{NA}}|$  behaves in almost the same fashion as the intrinsic entropy perturbation both before and after the transition, a feature that has been noticed earlier [31]. While they both behave as  $e^{-(2N)}$  at super-Hubble scales before the transition, they die down *extremely* rapidly (roughly as  $e^{-(80N)}$ !) during the radiation dominated epoch. It is these behavior which ensure that the amplitude of the total curvature perturbation remains unaffected.

<sup>2</sup> The amplitude of the non-adiabatic pressure perturbations corresponding to the cosmological scales (i.e.  $10^{-4} \lesssim k \lesssim 1 \text{ Mpc}^{-1}$ ) prove to be very small when they are well outside the Hubble radius. As a result, evolving these reliably until the transition to the radiation dominated epoch requires considerable numerical accuracy, which is difficult to achieve. For this reason, to illustrate the evolution of the non-adiabatic pressure perturbations, we choose to work with a very small scale mode that leaves the Hubble radius close to the end of inflation. Since the inflationary epoch is of the slow roll type for all the  $e$ -folds, the non-adiabatic pressure perturbations associated with the cosmological scales can be expected to behave in a fashion similar to that associated with such a small scale mode.

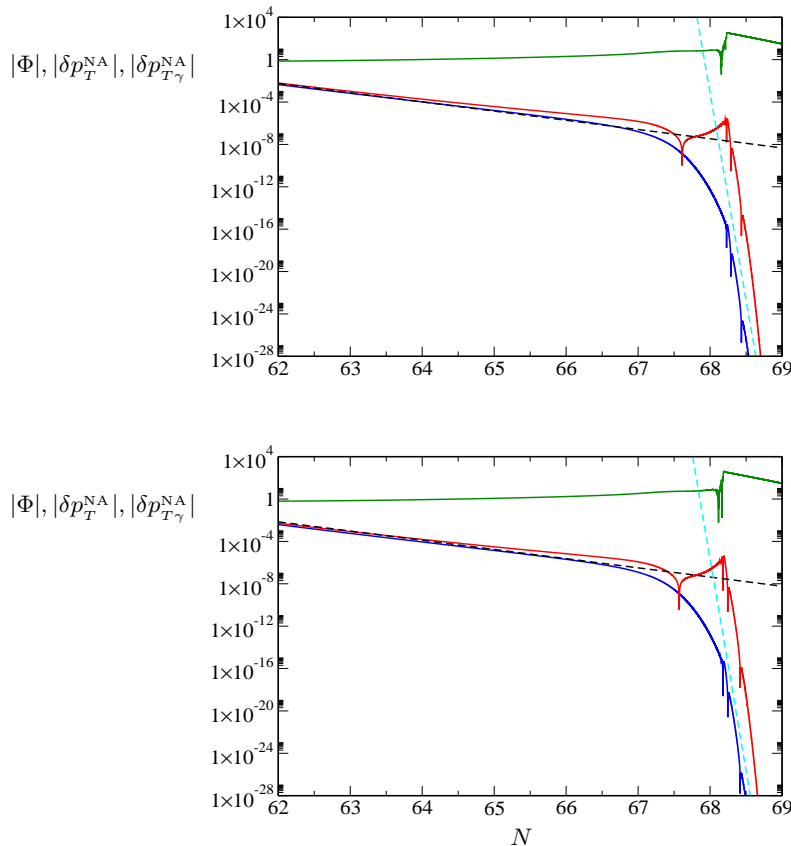


FIG. 3: The evolution of the amplitudes of the Bardeen potential  $|\Phi|$  (in green), the intrinsic entropy perturbation  $|\delta p_T^{\text{NA}}|$  (in blue) and the isocurvature perturbation  $|\delta p_{T\gamma}^{\text{NA}}|$  (in red) has been plotted as a function of the number of  $e$ -folds  $N$  for the two cases of  $\Gamma$ , as in the previous two figures. For computational reasons, we have chosen a very small scale mode with wavenumber  $k = 10^{16} \text{ Mpc}^{-1}$  that exits the Hubble radius during inflation around 58  $e$ -folds or so. Also, we have normalized the values of all the three quantities to be unity at Hubble exit. Clearly, while the Bardeen potential remains nearly a constant across the transition, both the intrinsic entropy and the isocurvature perturbations decay in almost the same fashion before as well as after the transition. The dashed lines in black and cyan indicate the  $e^{-2N}$  and  $e^{-80N}$  behavior, respectively. Interestingly, the non-adiabatic pressure perturbations die down extraordinarily rapidly after reheating is complete. It is these decay which ensure that the amplitude of the total curvature perturbation remains unaffected. Note that these plots correspond to the potential  $V_1(T)$  with values for the various parameters and the initial conditions that we have used in the last two figures. As in the earlier figures, we find that a very similar behavior occurs for the potential  $V_2(T)$ .

## V. SUMMARY AND DISCUSSION

In this work, we have studied the evolution of perturbations in an interacting system consisting of a tachyon and radiation. Treating the tachyon as an inflaton, we have investigated the effects of reheating—i.e. the perturbative transfer of energy from the tachyon to radiation—on the large scale curvature perturbations. We have shown that the transition does not alter the amplitude of the total curvature perturbation of the system when the rate describing the decay of the inflaton into radiation is either a constant or a function of the tachyon. We have also illustrated that, before the transition to the radiation dominated epoch, the relative non-adiabatic pressure perturbation between the tachyon and radiation decays in a fashion very similar to that of the intrinsic entropy perturbation associated with the tachyon. Moreover, we have shown that, after the transition, the relative non-adiabatic pressure perturbation between the tachyon and radiation dies down extremely rapidly during the early stages of the radiation dominated epoch. It is these behavior which ensure that the amplitude of the curvature perturbations remain unaffected during reheating.

It may be considered an overkill to integrate the second order differential equations rather than work with the much simpler first order equations [11, 27, 28]. Our motivations were threefold. Importantly, our effort allowed us to

cross-check certain previous results [11]. Also, our aim is to later study the effects of deviations from slow roll inflation as well as the effects of the modified dynamics close to the transition to the radiation dominated epoch on the small scale perturbations. As we had mentioned in the introduction, these effects can have interesting implications for the number density of primordial black holes that are formed towards the end of inflation [7]. Moreover, in possibilities such as the warm inflationary scenario, the decay rate, in addition to depending on the inflaton, can also depend on the temperature (see, for example, Refs. [25, 26, 32]). In such a case, the transfer of the energy from the inflaton to radiation may affect the amplitude and possibly the spectral index as well [17].

We would like to conclude by commenting on our choice for  $\Gamma(T)$ . As we had pointed out earlier, our choices were motivated by convenience in numerical evolution rather than physics. Obviously, better motivated functional forms of these quantities need to be investigated. We are currently exploring such issues.

### Acknowledgments

We would like to thank Raul Abramo, Sudipta Das, Ruth Durrer, Lev Kofman, Andrew Liddle, Misao Sasaki, Ashoke Sen and David Wands for valuable discussions. We would also like to acknowledge the use of the cluster computing facilities at the Harish-Chandra Research Institute, Allahabad, India, and at the Korea Institute for Advanced Study (KIAS), Seoul, Korea. R.K.J also wishes to thank KIAS for hospitality, where part of this work was carried out.

### Appendix A: The case of the canonical scalar field and a perfect fluid

In this appendix, we shall illustrate the corresponding effects for the case of the canonical scalar field model that was considered recently in the literature [16]. We shall rapidly summarize the essential equations describing the background evolution and the perturbations, and present the results.

#### 1. Background equations

In the case of a canonical scalar field, say,  $\phi$ , that is interacting with a perfect fluid, if one assumes that  $Q_F = (\Gamma \dot{\phi}^2)$ , then Eq. (6) that describes the conservation of the energy density of the fluid is given by

$$\dot{\rho}_F + 3H(1 + w_F)\rho_F = \Gamma \dot{\phi}^2. \quad (\text{A1})$$

Then, Eq. (7) implies that  $Q_\phi = -Q_F = -(\Gamma \dot{\phi}^2)$  and, hence, the continuity equation governing the energy density  $\rho_\phi$  of the scalar field reduces to

$$\dot{\rho}_\phi + 3H(\rho_\phi + p_\phi) = -\Gamma \dot{\phi}^2, \quad (\text{A2})$$

where  $p_\phi$  denotes the pressure of the field. The energy density and pressure associated with the canonical scalar field are given by

$$\rho_\phi = \frac{1}{2}\dot{\phi}^2 + V(\phi) \quad \text{and} \quad p_\phi = \frac{1}{2}\dot{\phi}^2 - V(\phi). \quad (\text{A3})$$

Upon using these expressions in the continuity equation (A2), we arrive at the following equation of motion governing the scalar field [15–17]:

$$\ddot{\phi} + 3H\dot{\phi} + \Gamma\dot{\phi} + V_\phi = 0, \quad (\text{A4})$$

where  $V_\phi \equiv (dV/d\phi)$ .

#### 2. Equations governing the scalar perturbations

Upon using the expressions for the perturbed energy density, momentum flux and pressure of the scalar field in Eq. (25), we can arrive at the equation of motion for the perturbation in the scalar field, say,  $\delta\phi$ , exactly as we did

for the perturbation in the tachyon. In the UCG, we find that  $\delta\phi$  satisfies the differential equation

$$\delta\ddot{\phi} + (3H + \Gamma) \delta\dot{\phi} + \left[ V_{\phi\phi} - \left( \frac{1}{a^2} \right) \nabla^2 \right] \delta\phi - \dot{\phi} \dot{A} + (2V_\phi + \Gamma \dot{\phi}) A - \left( \frac{\dot{\phi}}{a} \right) (\nabla^2 B) + \dot{\phi} \delta\Gamma = 0, \quad (\text{A5})$$

where  $V_{\phi\phi} = (d^2 V/d\phi^2)$  and, as before,  $\delta\Gamma$  denotes the first order perturbation in the decay rate. Again, on using Eq. (25), we find that the equation describing the conservation of the perturbed energy density of the fluid  $\delta\rho_F$  can be written as

$$\delta\dot{\rho}_F + 3H(1 + w_F) \delta\rho_F + \left( \frac{1}{a^2} \right) \nabla^2 \psi_F - 2\Gamma \dot{\phi} \delta\dot{\phi} + \Gamma \dot{\phi}^2 A - \left[ \frac{(1 + w_F) \rho_F}{a} \right] (\nabla^2 B) - \dot{\phi}^2 \delta\Gamma = 0. \quad (\text{A6})$$

Also, from the first order Einstein's equations (19) and (20), we can arrive at the following differential equation for the quantity  $\psi_F$  that describes the spatial velocity of the fluid:

$$\dot{\psi}_F + 3H\psi_F + w_F \delta\rho_F + (1 + w_F) \rho_F A + \Gamma \dot{\phi} \delta\phi = 0. \quad (\text{A7})$$

The perturbation variables that we shall evolve numerically are  $\mathcal{Q}_\phi = \delta\phi$  and the quantity  $\mathcal{Q}_F$  that we had introduced earlier [cf. Eq. (29)]. As in the case of the tachyon and the perfect fluid, using the background equations, the first order Einstein's equations for the system and the energy conservation equations for the scalar field and the fluid, we can arrive at the coupled second order differential equations (30) for  $\mathcal{Q}_\phi$  and  $\mathcal{Q}_F$ , with  $(\alpha, \beta) = (\phi, F)$  [16]. For the case wherein the decay rate  $\Gamma$  is a constant, the coefficients  $\mathcal{F}_{\alpha\beta}$  and  $\mathcal{G}_{\alpha\beta}$  are now given by

$$\mathcal{F}_{\phi\phi} = (3H + \Gamma), \quad (\text{A8})$$

$$\mathcal{F}_{\phi F} = \left( \frac{4\pi G}{H} \right) \left( \frac{w_F - 1}{w_F} \right) \dot{\phi} \sqrt{(1 + w_F) \rho_F}, \quad (\text{A9})$$

$$\mathcal{F}_{F\phi} = \left( \frac{4\pi G}{H} \right) \dot{\phi} (1 - w_F) \sqrt{(1 + w_F) \rho_F} + (1 + 2w_F) \left( \frac{\Gamma \dot{\phi}}{\sqrt{(1 + w_F) \rho_F}} \right), \quad (\text{A10})$$

$$\mathcal{F}_{FF} = 3H + \left( \frac{\Gamma \dot{\phi}^2}{\rho_F} \right), \quad (\text{A11})$$

$$\begin{aligned} \mathcal{G}_{\phi\phi} &= V_{\phi\phi} - \left( \frac{1}{a^2} \right) \nabla^2 + \left( \frac{4\pi G}{H} \right) \left[ 4V_\phi \dot{\phi} + 2(3H + \Gamma) \dot{\phi}^2 - \left( \frac{\Gamma \dot{\phi}^2}{\rho_F} \right) \right] \\ &\quad - \left( \frac{4\pi G}{H} \right)^2 \dot{\phi}^2 \left[ 2\dot{\phi}^2 + \left( \frac{(1 + w_F)^2}{w_F} \right) \rho_F \right], \end{aligned} \quad (\text{A12})$$

$$\begin{aligned} \mathcal{G}_{\phi F} &= \left( \frac{4\pi G}{H} \right) \left[ - \left( \frac{3H \dot{\phi}}{2} \right) \left( \frac{(1 + w_F)^2}{w_F} \right) + \left( \frac{1}{2\rho_F} \right) \left( \frac{w_F - 1}{w_F} \right) \Gamma \dot{\phi}^3 - 2V_\phi - \Gamma \dot{\phi} \right] \sqrt{(1 + w_F) \rho_F} \\ &\quad + \left( \frac{4\pi G}{H} \right)^2 \dot{\phi} \left[ 2\dot{\phi}^2 + \left( \frac{(1 + w_F)^2}{w_F} \right) \rho_F \right] \sqrt{(1 + w_F) \rho_F}, \end{aligned} \quad (\text{A13})$$

$$\begin{aligned} \mathcal{G}_{F\phi} &= - \left( \frac{4\pi G}{H} \right) \left[ V_\phi (1 + w_F)^2 \rho_F + 3H V_\phi \dot{\phi} (1 + w_F)^2 \rho_F - \Gamma \dot{\phi}^3 \right] \left( \frac{1}{\sqrt{(1 + w_F) \rho_F}} \right) \\ &\quad + \left( \frac{4\pi G}{H} \right)^2 (\dot{\phi}^2 + 2\rho_F) \left( \frac{(1 + w_F^2) \rho_F \dot{\phi}}{\sqrt{(1 + w_F) \rho_F}} \right) - \left( \frac{\Gamma}{\sqrt{(1 + w_F) \rho_F}} \right) (V_\phi - 3H w_F \dot{\phi} + \Gamma \dot{\phi}), \end{aligned} \quad (\text{A14})$$

$$\begin{aligned} \mathcal{G}_{FF} &= - \left( \frac{w_F}{a^2} \right) \nabla^2 + \left( \frac{9H^2}{4} \right) (1 - w_F^2) \\ &\quad + \left( \frac{4\pi G}{H} \right) \left[ \left( \frac{3H}{2} \right) (1 + w_F) (1 + 3w_F) \rho_F + \left( \frac{3H}{2} \right) \dot{\phi}^2 (w_F - 1) - \Gamma \dot{\phi}^2 \right] \\ &\quad - \left( \frac{4\pi G}{H} \right)^2 \left[ (1 + w_F)^2 \rho_F \dot{\phi}^2 + 2((1 + w_F) \rho_F)^2 \right] - \left( \frac{\Gamma \dot{\phi}}{\rho_F} \right) \left[ V_\phi + \Gamma \dot{\phi} - \left( \frac{3H}{2} \right) w_F \dot{\phi} + \left( \frac{\Gamma \dot{\phi}^3}{4\rho_F} \right) \right]. \end{aligned} \quad (\text{A15})$$



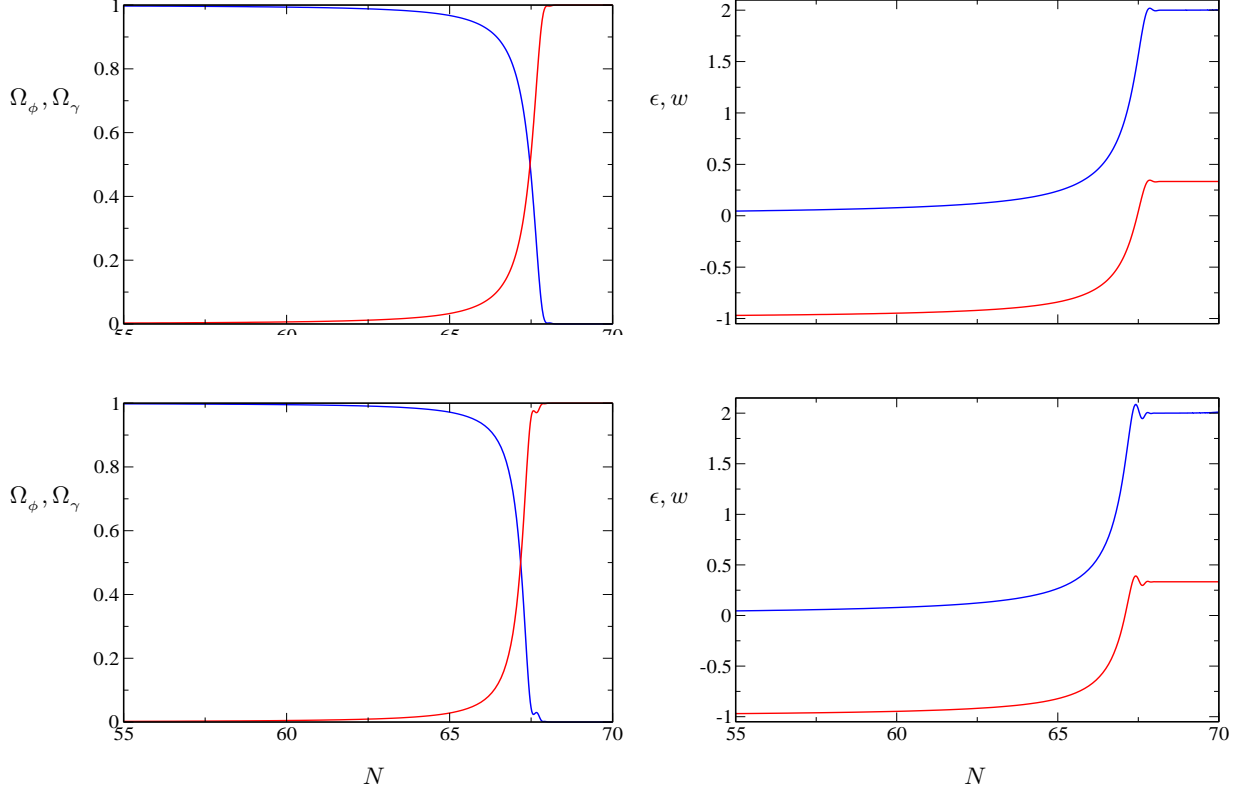


FIG. 4: In the left column, the evolution of the quantities  $\Omega_\phi$  (in blue) and  $\Omega_\gamma$  (in red) has been plotted as a function of the number of  $e$ -folds  $N$  for the two types of  $\Gamma$ , as discussed in the earlier figures. In the right column, we have plotted the evolution of the first Hubble slow roll parameter  $\epsilon$  (in blue) and the equation of state parameter  $w$  of the entire system (in red). We have considered the popular quadratic potential to describe the scalar field, and we have worked with suitable parameters and initial condition to arrive at the required behavior. These plots clearly illustrate the transfer of energy from the inflaton to radiation. We should point out that the oscillations in the plots arise due to the oscillations by the field at the bottom of the potential, a feature that does not arise in the case of the tachyon.

For the case wherein the decay rate is a function of the scalar field, the coefficients  $\mathcal{G}_{\phi\phi}$  and  $\mathcal{G}_{F\phi}$  are modified to

$$\mathcal{G}_{\phi\phi} \rightarrow \mathcal{G}_{\phi\phi} + \dot{\phi} \Gamma_\phi, \quad (\text{A16})$$

$$\mathcal{G}_{F\phi} \rightarrow \mathcal{G}_{F\phi} + \left( \frac{w_F}{\sqrt{(1+w_F) \rho_F}} \right) \dot{\phi}^2 \Gamma_\phi, \quad (\text{A17})$$

where  $\Gamma_\phi \equiv (d\Gamma/d\phi)$ . The other coefficients remain unchanged.

### 3. Results

In Fig. 4, we have illustrated the transition from inflation to the radiation dominated epoch by plotting the dimensionless energy density parameters  $\Omega_\phi$  and  $\Omega_\gamma$  for the two possible types of decay. We have also plotted the evolution of the first Hubble slow roll parameter  $\epsilon$  and the equation of state parameter  $w$  for the entire system. Note that we have considered the quadratic potential  $V(\phi) = (m^2 \phi^2/2)$ , and have chosen suitable values for the parameters and initial conditions to achieve the desired behavior. And, in Fig. 5, as in the case of the tachyon discussed in the text, we have plotted the evolution of the amplitudes of the individual and the total curvature perturbations, as well as the scalar power spectrum before and after the transition. It is evident from these two figures that the conclusions

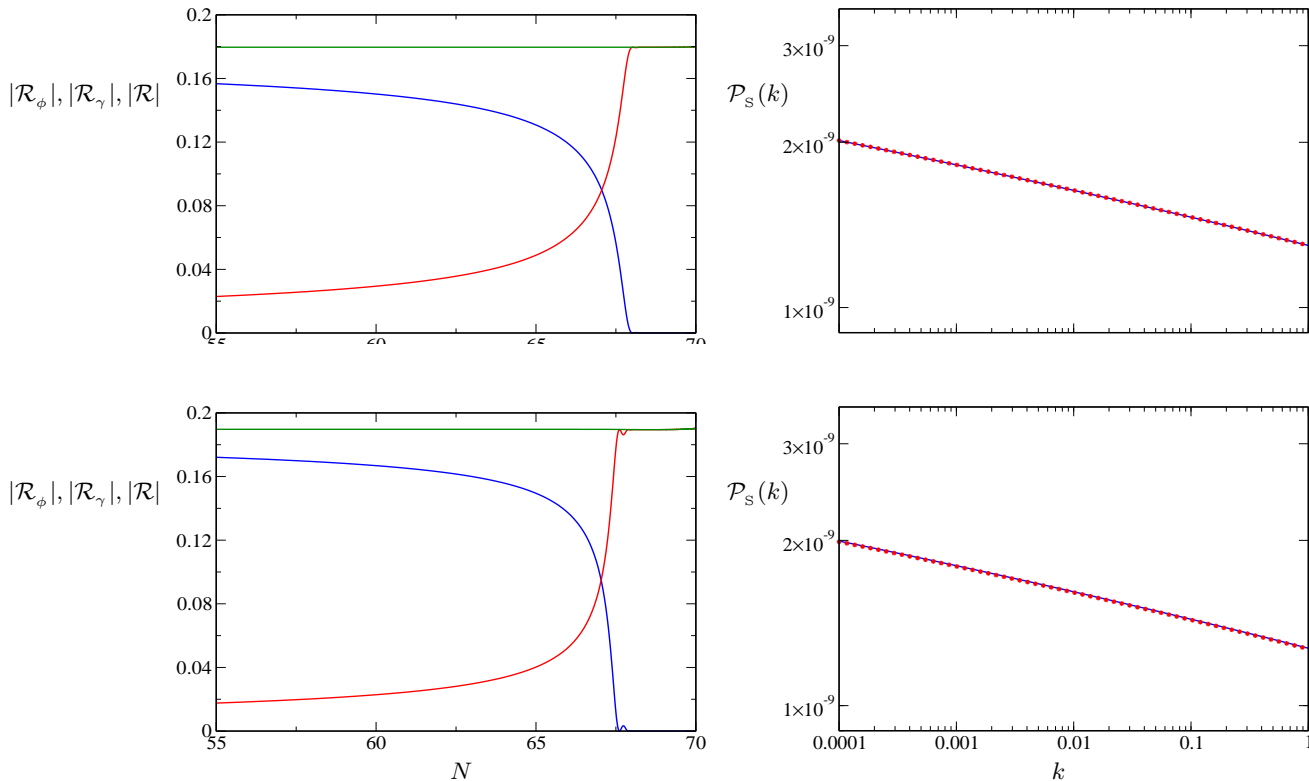


FIG. 5: In the left column, the evolution of the amplitudes of the curvature perturbations associated with the scalar field ( $|\mathcal{R}_\phi|$ , in blue), radiation ( $|\mathcal{R}_\gamma|$ , in red) and the total curvature perturbation of the entire system ( $|\mathcal{R}|$ , in green) has been plotted as a function of the number of  $e$ -folds  $N$  for the two types of the decay rate. For illustration, we have again chosen a typical cosmological mode with wavenumber  $k = 0.01 \text{ Mpc}^{-1}$ . In the right column, as before, we have plotted the scalar power spectrum before (in blue) and after (in red) the transition. It is evident that, as in the case of the tachyon, the amplitude of the nearly scale invariant power spectrum remains unaffected for both types of the decay rate.

we had arrived at for the tachyon apply equally well to the case involving the canonical scalar field as well.

- 
- [1] E. W. Kolb and M. S. Turner, *The Early Universe* (Addison-Wesley, Redwood City, California, 1990); A. R. Liddle and D. H. Lyth, *Cosmological Inflation and Large-Scale Structure* (Cambridge University Press, Cambridge, England, 1999); V. F. Mukhanov, *Physical Foundations of Cosmology* (Cambridge University Press, Cambridge, England, 2005); R. Durrer, *The Cosmic Microwave Background* (Cambridge University Press, Cambridge, England, 2008).
  - [2] H. Kodama and M. Sasaki, *Prog. Theor. Phys. Suppl.* **78**, 1 (1984); V. F. Mukhanov, H. A. Feldman and R. H. Brandenberger, *Phys. Rep.* **215**, 203 (1992); J. E. Lidsey, A. Liddle, E. W. Kolb, E. J. Copeland, T. Barreiro and M. Abney, *Rev. Mod. Phys.* **69**, 373 (1997); B. Bassett, S. Tsujikawa and D. Wands, *Rev. Mod. Phys.* **78**, 537 (2006); K. A. Malik and D. Wands, *Phys. Rept.* **475**, 1 (2009).
  - [3] S. M. Leach and A. R. Liddle, *Phys. Rev. D* **63**, 043508 (2001); S. M. Leach, M. Sasaki, D. Wands and A. R. Liddle, *Phys. Rev. D* **64**, 023512 (2001).
  - [4] R. K. Jain, P. Chingangbam and L. Sriramkumar, *JCAP* **0710**, 003 (2007).
  - [5] E. Bugaev and P. Klimai, *Phys. Rev. D* **78**, 063515 (2008).
  - [6] H. M. Hodges, G. R. Blumenthal, L. A. Kofman and J. R. Primack, *Nucl. Phys. B* **335**, 197 (1990); V. F. Mukhanov and M. I. Zelnikov, *Phys. Lett. B* **263**, 169 (1991); A. A. Starobinsky, *Sov. Phys. JETP Lett.* **55**, 489 (1992); J. A. Adams, G. G. Ross and S. Sarkar, *Nucl. Phys. B* **503**, 405 (1997); J. Lesgourgues, *Nucl. Phys. B* **582**, 593 (2000); J. Barriga, E. Gaztanaga, M. Santos and S. Sarkar, *Mon. Not. Roy. Astron. Soc.* **324**, 977 (2001); *Nucl. Phys. Proc. Suppl.* **95**, 66 (2001); J. A. Adams, B. Cresswell, R. Easther, *Phys. Rev. D* **64**, 123514 (2001); B. Feng and X. Zhang, *Phys. Lett. B* **570**, 145 (2003); C. R. Contaldi, M. Peloso, L. Kofman and A. Linde, *JCAP* **0307**, 002 (2003); J. M. Cline, P. Crotty and J. Lesgourgues, *JCAP* **0309**, 010 (2003); P. Hunt and S. Sarkar, *Phys. Rev. D* **70**, 103518 (2004); *ibid.* **76**, 123504 (2007);

- J.-O. Gong, JCAP **0507**, 015 (2005); R. Sinha and T. Souradeep, Phys. Rev. D **74**, 043518 (2006); L. Covi, J. Hamann, A. Melchiorri, A. Slosar and I. Sorbera, Phys. Rev. D **74**, 083509 (2006); J. Hamann, L. Covi, A. Melchiorri and A. Slosar, Phys. Rev. D **76**, 023503 (2007); D. Boyanovsky, H. J. de Vega and N. G. Sanchez, Phys. Rev. D **74**, 123006 (2006); *ibid* **74**, 123007 (2006); B. A. Powell and W. H. Kinney, Phys. Rev. D **76**, 063512 (2007); G. Nicholson and C. R. Contaldi, JCAP **0801**, 002 (2008); M. Joy, V. Sahni, A. A. Starobinsky, Phys. Rev. D **77**, 023514 (2008); M. Joy, A. Shafieloo, V. Sahni, A. A. Starobinsky, JCAP **0906**, 028 (2009); C. Destri, H. J. de Vega and N. G. Sanchez, Phys. Rev. D **78**, 023013 (2008); R. K. Jain, P. Chingangbam, J.-O. Gong, L. Sriramkumar and T. Souradeep, JCAP **0901**, 009 (2009); R. K. Jain, P. Chingangbam, L. Sriramkumar and T. Souradeep, Phys. Rev. D **82**, 023509 (2010); D. K. Hazra, M. Aich, R. K. Jain, L. Sriramkumar and T. Souradeep, JCAP **1010**, 008 (2010).
- [7] I. Zaballa, A. M. Green, K. A. Malik and M. Sasaki, JCAP **0703**, 010 (2007); S. Chongchitnan and G. Efstathiou, JCAP **0701**, 011 (2007); K. Kohri, D. H. Lyth and A. Melchiorri, JCAP **0804**, 038 (2008); R. Saito, J. Yokoyama and R. Nagata, JCAP **0806**, 024 (2008).
- [8] J. H. Traschen and R. Brandenberger, Phys. Rev. D **42**, 2491 (1990); A. D. Dolgov and D. P. Kirilova, Sov. J. Nucl. Phys. **51**, 172 (1990); L. Kofman, A. D. Linde and A. A. Starobinsky, Phys. Rev. Lett. **73**, 3195 (1994); Y. Shtanov, J. H. Traschen and R. H. Brandenberger, Phys. Rev. D **51**, 5438 (1995); L. Kofman, A. D. Linde and A. A. Starobinsky, Phys. Rev. D **56**, 3258 (1997); B. A. Bassett and F. Tamburini, Phys. Rev. Lett. **81**, 2630 (1998); B. A. Bassett, C. Gordon, R. Maartens and D. I. Kaiser, Phys. Rev. D **61**, 061302(R) (2000); B. A. Bassett and F. Viniegra, *ibid.* **62**, 043507 (2000); B. A. Bassett and S. Tsujikawa, *ibid.* **63**, 123503 (2001); P. Ivanov, Phys. Rev. D **61**, 023505 (1999); F. Finelli and R. Brandenberger, Phys. Rev. Lett. **82**, 1362 (1999); Phys. Rev. D **62**, 083502 (2000); R. Easther and M. Parry, Phys. Rev. D **62**, 103503 (2000); S. Tsujikawa and B. A. Bassett, Phys. Lett. B **536**, 9 (2002).
- [9] T. Suyama and S. Yokoyama, Class. Quant. Grav. **24**, 1615 (2007); P. R. Anderson, C. Molina-Paris, D. Evanich and G. B. Cook, Phys. Rev. D **78**, 083514 (2008); D. Battefeld and S. Kawai, Phys. Rev. D **77**, 123507 (2008); D. Battefeld, Nucl. Phys. Proc. Suppl. **192-193**, 126 (2009).
- [10] D. H. Lyth and D. Wands, Phys. Lett. B **524**, 5 (2002); D. H. Lyth, C. Ungarelli and D. Wands, Phys. Rev. D **67**, 023503 (2003).
- [11] S. Matarrese and A. Riotto, JCAP **0308**, 007 (2003).
- [12] A. Mazumdar and M. Postma, Phys. Lett. B **573**, 5 (2003).
- [13] S. Tsujikawa, Phys. Rev. D **68**, 083510 (2003); G. Dvali, A. Gruzinov and M. Zaldarriaga, Phys. Rev. D **69**, 023505 (2004).
- [14] K. Dimopoulos and D. H. Lyth, Phys. Rev. D **69**, 123509 (2004).
- [15] A. Albrecht, P. J. Steinhardt, M. S. Turner and F. Wilczek, Phys. Rev. Lett. **48**, 1437 (1982); M. S. Turner, Phys. Rev. D **28**, 1243 (1983); E. W. Kolb, A. Notari and A. Riotto, Phys. Rev. D **68**, 123505 (2003).
- [16] F. Di Marco, F. Finelli and A. Gruppuso, Phys. Rev. D **76**, 043530 (2007).
- [17] A. Cerioni, F. Di Marco, F. Finelli and A. Gruppuso, Phys. Rev. D **78**, 021301(R) (2008).
- [18] A. Sen, JHEP **9910**, 008 (1999); M. Garousi, Nucl. Phys. B **584** 284, (2000); E. Bergshoeff, M. de Roo, T. de Wit, E. Eyras and S. Panda, JHEP **0005**, 009 (2000); J. Kluson, Phys. Rev. D **62**, 126003 (2000).
- [19] A. Sen, JHEP **0204**, 048 (2002); JHEP **0207**, 065 (2002).
- [20] M. Sami, P. Chingangbam and T. Qureshi, Phys. Rev. D **66**, 043530 (2002).
- [21] D. A. Steer and F. Vernizzi, Phys. Rev. D **70**, 043527 (2004).
- [22] P. Chingangbam, S. Panda and A. Deshamukhya, JHEP **0502**, 052 (2005).
- [23] C. Campuzano, S. del Campo and R. Herrera, Phys. Rev. D **72**, 083515 (2005); Phys. Lett. B **633**, 149 (2006); JCAP **0606** 017, (2006).
- [24] V. H. Cardenas, Phys. Rev. D **73**, 103512 (2006).
- [25] R. Herrera, S. del Campo and C. Campuzano, JCAP **0610**, 009 (2006); S. del Campo, R. Herrera and J. Saavedra, Eur. Phys. J. C **59**, 913 (2009).
- [26] M. Bastero-Gil and A. Berera, Int. J. Mod. Phys. A **24**, 2207 (2009).
- [27] K. A. Malik, D. Wands and C. Ungarelli, Phys. Rev. D **67**, 063516 (2003).
- [28] K. A. Malik, arXiv:astro-ph/0101563.
- [29] K. A. Malik and D. Wands, JCAP **0502**, 007 (2005).
- [30] C. Gordon, D. Wands, B. A. Bassett and R. Maartens, Phys. Rev. D **63**, 023506 (2001).
- [31] N. Bartolo, P. S. Corasaniti, A. R. Liddle and M. Malquarti, Phys. Rev. D **70**, 043532 (2004).
- [32] A. Deshamukhya and S. Panda, Int. J. Mod. Phys. D **18**, 2093 (2009).